Available online at www.sciencedirect.com
ScienceDirect
Carbohydrate Polymers 67 (2007) 511–529
Carbohydrate Polymers
www.elsevier.com/locate/carbpol

A new insight into the gelatinization process of native starches ☆

Wajira S. Ratnayake, David S. Jackson *

Department of Food Science and Technology, University of Nebraska-Lincoln, Lincoln, NE 68583-0919, USA

Received 25 March 2006; received in revised form 13 June 2006; accepted 19 June 2006
Available online 1 August 2006

Abstract

The gelatinization characteristics of seven different food starches (regular corn, high-amylose corn, waxy corn, wheat, rice, potato, and tapioca) were investigated. Each starch sample type was heated to 35, 40, 45, etc. up to 85 °C at 5 °C intervals, and freeze-dried. The treated samples were analyzed using light microscopy, scanning electron microscopy (SEM), differential scanning calorimetry (DSC), X-ray diffraction (XRD), and high-performance size exclusion chromatography (HPSEC). When heated, granules underwent structural changes prior to the visible morphological changes that took place during gelatinization. The nature of these structural changes depended on starch type. These results indicate that the starch gelatinization process is more complex than a simple granular order-to-disorder transition.

Keywords: Starch; Gelatinization; Phase transition

1. Introduction

Starch is the most common carbohydrate polymer in foods. A proper understanding of starch phase transitions or gelatinization is extremely important in food processing operations (Roos, 1995).

Starch gives two distinct endotherms during gelatinization at low water contents. Donovan (1979) reported that these endotherms were due to phase transitions, which were governed by the degree to which ordered regions within granules were hydrated. The high temperature transition is due to melting of crystallites without adequate moisture. When excess water is present, the high temperature transition disappears. Donovan (1979) further reported that, at high water contents, the amorphous regions of the granules imbibed water and swelled, resulting in stripping or separation of starch chains from portions of these crystallites. When all crystals are stripped at high moisture levels, there would not be any crystallites remaining to be melted at high temperature (Donovan, 1979).

Evans and Haisman (1982) proposed the "cooperative melting theory" which explained the bi-phasic endotherm as a result of crystallite stability within the granules. The granules containing least stable crystallites start to change first upon heating. Water absorption by the granules lowers the melting points of crystallites, which results in quick melting of remaining crystallites. This process reduces the constraints of still remaining crystallites to lower their melting points. This cooperative process happens quickly when there is sufficient water and gives a narrow or single DSC endotherm. At low water contents, however, there is not sufficient water for cooperative melting to take place. This results in a second endotherm (or a "shoulder" depending on the water content), which represents crystallites melting after the cooperative process, at a higher temperature (Evans & Haisman, 1982).

Abbreviations: ΔH, enthalpy (by differential scanning calorimetry); CPS, counts per second; DSC, differential scanning calorimetry; HPSEC, high-performance size exclusion chromatography; SD, standard deviation; SEM, scanning electron microscopy; T_c, DSC conclusion (or end) temperature; T_g, glass transition temperature; T_o, DSC onset temperature; T_p, DSC peak temperature; XRD, X-ray diffraction.

☆ A contribution of the University of Nebraska Agricultural Research Division, Lincoln, NE 68583, USA. Journal Series No. 15173.

* Corresponding author. Tel.: +1 402 472 2814; fax: +1 402 472 1693.
E-mail address: djackson@unlnotes.unl.edu (D.S. Jackson).

0144-8617/$ - see front matter © 2006 Elsevier Ltd. All rights reserved.
doi:10.1016/j.carbpol.2006.06.025

Nakazawa, Noguchi, and Takahashi (1984) concluded, by annealing studies, that the biphasic endotherm at low moisture contents was due to the melting of starch polymers in amorphous regions (low temperature endotherm) followed by crystalline regions melting (high temperature endotherm). They observed a decrease in enthalpy with increasing annealing temperature for 45 h. However, other investigators observed either no difference (Qi, Tester, Snape, & Ansell, 2005) or an increase (Marchant & Blanshard, 1978) in enthalpy in annealed starch.

Biliaderis, Page, Maurice, and Juliano (1986) proposed a new three-phase ((1) fully ordered crystalline phase, (2) non-ordered intercrystalline phase, and (3) bulk amorphous phase) model, as opposed to traditional two-phase (amorphous and crystalline phases) model, for starch structures to help explain the gelatinization process. They argued that their three-phase model better described the multiple melting profiles observed during starch gelatinization at low moisture levels and that the gelatinization process involved partial melting, recystallization, and final complete melting of crystallites.

Jenkins and Donald (1998) reported that changes in crystallinity during gelatinization processes occurred both prior to the onset (T_o) and after the endotherm conclusion temperatures (T_c). More than 20% of total crystallinity, as revealed by XRD, remained after wheat, potato, corn, tapioca, and pea starches were heated past T_c. Based on these observations, Jenkins and Donald (1998) concluded that differential scanning calorimetry (DSC) did not explain all changes that take place during gelatinization and that gelatinization occurred over a wider temperature range than what is indicated by DSC endotherms.

Sahai and Jackson (1999) observed a lowering of onset and peak temperatures and an increase in end temperature of endotherms at low (50%) moisture levels. They argued that there was an increased facilitation of lower stability crystallite melting and an increased temperature stability of the more stable crystallites. These phenomena were not adequately explained by the starch gelatinization models proposed by Donovan (1979) and Evans and Haisman (1982). Investigations on annealed starch (Sahai & Jackson, 1999) suggested that disappearance of the second endotherm in annealed starch contradicted the model proposed by Biliaderis et al. (1986). Considering the available accumulated evidence, Sahai and Jackson (1999) and Fukuoka et al. (2002) suggested that starch granule enthalpic transitions, at various moisture levels, did not represent a single phenomenon, but instead represented a number of different changes that occur simultaneously. Moreover, different techniques used to measure gelatinization parameters give slightly different results (Liu, Charlet, Yelle, & Arul, 2002) indicating either that different changes occur during the measurement process or that there are limitations to the particular technique being used.

The objective of this study was to investigate progressive changes in granular and molecular structures in different food starches during the gelatinization process. The seven samples used in this study are used widely in the food industry and represent all three structural polymorphism categories of food starches (A – corn [*Zea mays* L.], rice [*Oryza sativa* L.], and wheat [*Triticum aestivum* L.]; B – potato [*Solanum tuberosum* L.]; and C – tapioca [*Manihot esculenta* Crantz]).

2. Materials and methods

Starch samples were obtained from commercial sources as follows: regular corn starch, high-amylose corn starch, and waxy corn starch from Cargill Inc. (Cedar Rapids, IA), potato and tapioca starches from Penford Food Ingredients Co. (Englewood, CO), rice starch from A and B Food Ingredients (Fairfield, NJ) and wheat starch from Archer Daniels Midland (ADM) Co. (Olathe, KS).

2.1. Sample treatment

Distilled water (100 mL) was heated to a specific temperature (35, 40, 45, etc., up to 85 °C at 5 °C intervals) in a Fisher Isotemp model 3028H circulator (Fisher Scientific Inc., Pittsburgh, PA). When water in the flask reached the desired temperature, a 6 g starch sample were added, mixed by hand swirling the contents, and held at that temperature for 30 min. The sample containing flasks were swirled by hand after 5, 10, and 20 min to resuspend precipitated starch.

After heat treatments, samples were filtered through Whatman No. 1 filter papers and the residues were freeze-dried in a Virtis Sentry 8L freeze-dryer (The Virtis Co., Gardiner, NY) for 36 h at −55 °C and 200 mTorr pressure.

2.2. Light microscopy

Untreated samples (~0.10 g in ~15 mL water) were heated to specific temperature in a glass Petri-dish on a regular electric laboratory hot-plate while monitoring the temperature with a non-contact infra-red thermometer. Upon reaching a designated temperature, sample in the petri dish was observed promptly using an Olympus Provis AX70 microscope (Olympus America Inc., Melville, NY) equipped with a 40× or 60× water immersion lens (400× or 600× magnification) and an Optronics (Optronics, Goleta, CA) camera attached to the eye piece. Digital images were captured using MagnaFire version 2.1C (Optronics, Goleta, CA) software.

2.3. Scanning electron microscopy (SEM)

Starch samples were mounted on metal stubs and coated with gold–palladium (~20 nm thickness) using a

Hummer sputter coating system (Anatech Ltd., Union City, CA). Samples were then observed using a Hitachi S-3000N scanning electron microscope (Hitachi Science Systems, Tokyo, Japan) at an acceleration potential of 15 kV. Pictures were captured by automatic image capturing software (Hitachi High-Technologies, Pleasanton, CA).

2.4. Differential scanning calorimetry (DSC)

Starch samples (~10 mg, db) with ~55 μL distilled water (i.e., starch in excess water) were hermetically sealed in DSC pans (Perkin Elmer Pan Sell Kit 0319-1525/1526/1535) and kept at room temperature for 2–3 h. Next, samples were scanned against a blank (empty pan) using a Perkin Elmer Pyris 1 DSC (Perkin-Elmer Co., Norwalk, CT) from 25 to 90 °C at a 10 °C/min scanning rate. Pyris version 3.52 (Perkin-Elmer Co., Norwalk, CT) software was used to collect data and analyze onset (T_o), peak (T_p), and end (T_c) temperatures, and the transition enthalpy (ΔH). Equipment was calibrated using indium as the reference material.

2.5. X-ray diffraction (XRD)

X-ray diffraction data were obtained using a Rigaku D/Max-B X-ray diffractometer (Rigaku Corporation, Tokyo, Japan) with Bragg–Brentano parafocusing geometry, a diffracted beam monochromator, copper target X-ray tube set to 40 KV and 30 mA. The other equipment settings were as follows: 1° divergence slit, 1° scatter slit, 0.3 mm receiving slit, 0.8 mm monochromator receiving slit, incident and diffracted beam Soller slits (angular aperture = 5°). The dry samples were mounted as a smooth-surfaced smear on zero-background quartz slides with a few drops of ethanol and allowed to air-dry at room temperature for approximately 20 min. The samples were then scanned from 3° to 35° in the diffractometer. Data were collected using Rigaku software (version 2.0) as counts per second (CPS) versus Bragg angle ($\theta/2\theta$).

Percent relative crystallinity was calculated according to the method by Nara, Mori, and Komiya (1978) using quartz as 100% crystalline material (Eliasson et al., 1987) and an 85 °C treated sample of each starch as 100% amorphous material. Peak fitting software Origin Version 6.0/SR-4 (Microcal Software Inc., Northhampton, MA, USA) was used to calculate absolute differences between XRD profiles. The percentage relative crystallinity was calculated as follows:

$$\%\text{Relative crystallinity} = \left(\sum |I_s - I_a| / \sum |I_c - I_a|\right) * 100\%$$

where, $|I_s - I_a|$ = absolute difference between the sample [I_s] and amorphous [I_a] intensities, and $|I_c - I_a|$ = absolute difference between the crystalline (quartz) [I_c] and amorphous [I_a] intensities.

2.6. High-performance size exclusion chromatography (HPSEC)

Samples of 0.5 g dry weight were dispersed in 100 mL of 90% (v/v) reagent grade DMSO (Mallinckrodt Baker Inc., Paris, KY) in water by keeping the mixture at room temperature for 5 days with vortex mixing for 10 s every 24 h (method developed following observations by Sene, Thevenot, & Prioul, 1997). HPSEC was carried out according to Ozcan and Jackson (2002) with slight modifications as follows: dispersed samples were passed through a 1.2 μm Magna nylon supported membrane (GE Osmonics Labstore, Minnetonka, MN) and 25 μL was injected into a

Table 1
Summary of light microscopic observations[a] of native starches heated in excess water

Temperature treatment (°C)	Starch type						
	Regular corn	Waxy corn	High-amylose corn	Wheat	Rice	Potato	Tapioca
35							
40							
45				a			
50				b	a		a
55	a	a		b	c	b, c	b, c
60	b	b, c	c	c	e	c	e
65	c	f	c	c	e	d	f
70	d	f	c	d	f	e	f
75	e	f	c	e	f	f	f
80	f	f	d	f	f	f	f
85	f	f	d	f	f	f	f

[a] The degree of granular disruption increases according to the alphabetical order of the letters in each column as follows: (blank space), No visible changes in the granular morphology; a, visible swelling in very few numbers of granules; b, a large number (more than 50%) of granules are swollen; c, few (less than 25%) granules are disrupted; d, approximately 50% of granules disrupted; e, very few (less than 10%) intact/swollen granules visible, the rest is disrupted; and f, all granules are disrupted.

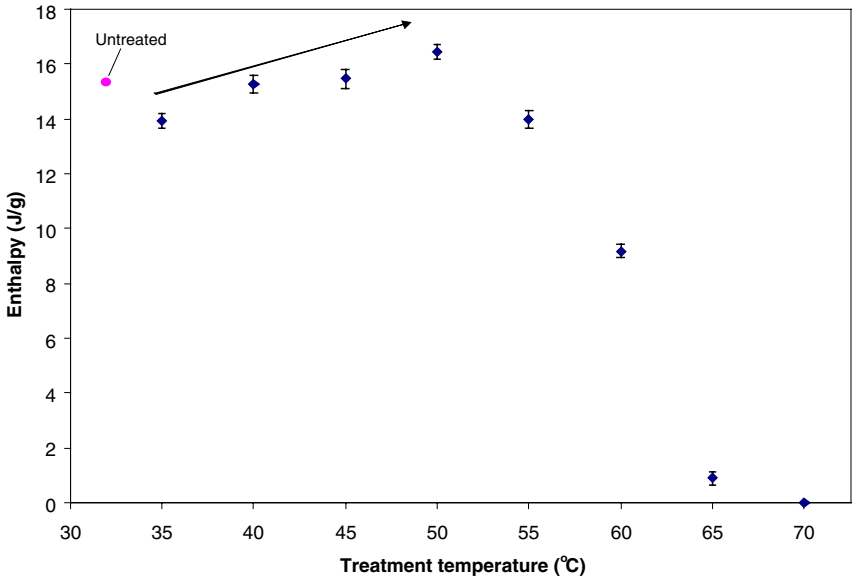

Fig. 1. Representative DSC enthalpies of regular corn starch samples heated to specific temperatures (each data point represents the mean and standard deviation of three independent replicates). Temperatures above 65 °C did not yield enthalpies.

Table 2
Relative amounts[a] of amylose dispersed in treated regular corn starch samples

Temperature treatment (°C)	Amylose (%)[b]
35	29.12 c
40	26.10 b
45	26.79 b, c
50	25.89 b
55	25.35 b
60	22.89 a
65	21.86 a
70	21.43 a
75	27.82 b
80	28.80 c
85	34.24 d

[a] In HPSEC profiles of regular corn starch, peak 1 (first peak on the left) represents amylopectin and peak 2 represents amylose. Peak 1 + Peak 2 = 100%.

[b] Numbers followed by the same letters are not significantly different by Tukey's HSD test ($p > 0.05$).

Table 3
Amylose and amylopectin molecular weights of treated starch samples

Starch type	Molecular weight ± SD	
	Amylopectin[a]	Amylose[a]
Regular corn starch	$1.21 \times 10^7 \pm 6.04 \times 10^5$	$1.12 \times 10^5 \pm 5.58 \times 10^3$
High-amylose corn starch	$1.40 \times 10^7 \pm 6.10 \times 10^5$	$5.28 \times 10^4 \pm 2.60 \times 10^3$
Waxy corn starch	$3.03 \times 10^7 \pm 1.21 \times 10^6$	None
Wheat starch	$1.12 \times 10^7 \pm 5.26 \times 10^5$	$1.43 \times 10^5 \pm 6.70 \times 10^3$
Rice starch	$1.49 \times 10^7 \pm 5.97 \times 10^5$	$6.17 \times 10^4 \pm 2.47 \times 10^3$
Potato starch	$4.66 \times 10^7 \pm 163 \times 10^5$	$2.06 \times 10^5 \pm 7.23 \times 10^3$
Tapioca starch	$2.60 \times 10^7 \pm 1.04 \times 10^6$	$2.39 \times 10^5 \pm 9.58 \times 10^3$

[a] There were no significant ($p < 0.05$) differences among different treatments within the same starch type.

HPSEC system equipped with a Waters 515 HPLC pump, Waters 410 differential refractometer (Waters Co., Milford, MA), Shodex KS- G, KS 806, 804, 803, and 802 columns

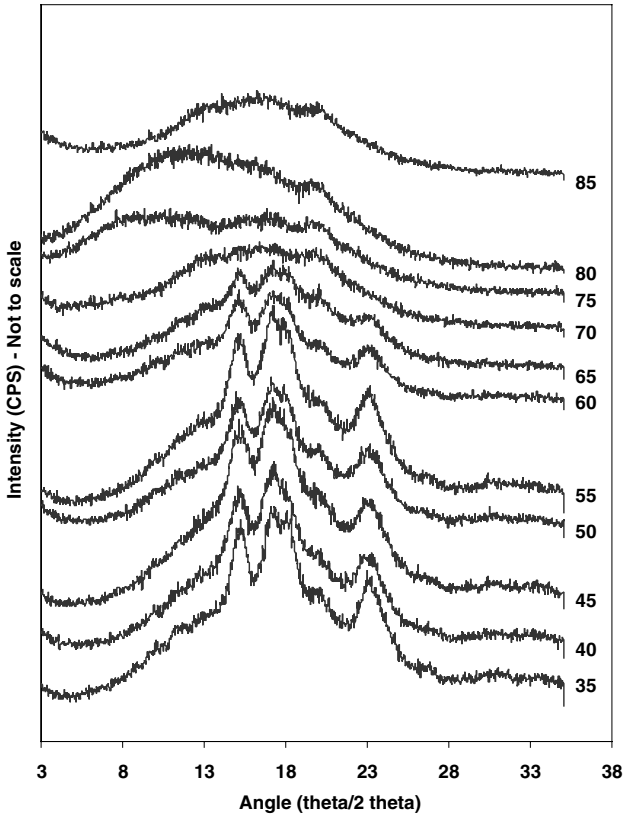

Fig. 2. Representative XRD patterns of regular corn starch. Numbers to the right of each profile represent the corresponding treatment temperature (°C).

(Showa Denko, Tokyo, Japan) connected in series and maintained at 50 °C. Distilled deionized degassed water was used as mobile phase with a 1 mL/min flow rate. Data were acquired automatically with Astra software Version 4.70.07 (Wyatt Technology Co., Santa Barbara, CA).

A molecular weight standard series was prepared using Shodex pullulan standards (Showa Denko K. K., Tokyo, Japan) P-5. P-10, P-20, P-50, P-100, P-200, P-400, and P-800 representing molecular weights 0.53×10^4, 1.2×10^4, 2.08×10^4, 4.67×10^4, 9.54×10^4, 19.4×10^4, 33.8×10^4, and 75.8×10^4, respectively. A standard curve was prepared by plotting log MW versus HPSEC peak retention time of each standard, and sample molecular weights were estimated using the following equation:

$$\log \mathrm{MW} = (42.15 - RT)/3.45 \quad [R^2 = 0.99],$$

where MW = molecular weight, and RT = retention time (min).

Relative peak areas (%) of amylose and amylopectin were estimated using Origin version 6.0 software (OriginLab Co., Northampton, MA)

2.7. Statistical analyses

All numerical results are averages of at least three independent replicates. The mean differences were determined by Tukey's HSD test ($p < 0.05$) using JMP 5.0.1.2 software (SAS Institute, Cary, NC).

3. Results and discussion

Representative DSC profiles of all treated samples of each starch type are given in the Appendices A1–A7. A summary of light microscopic observations is given in Table 1. Representative HPSEC profiles are shown in Appendix B.

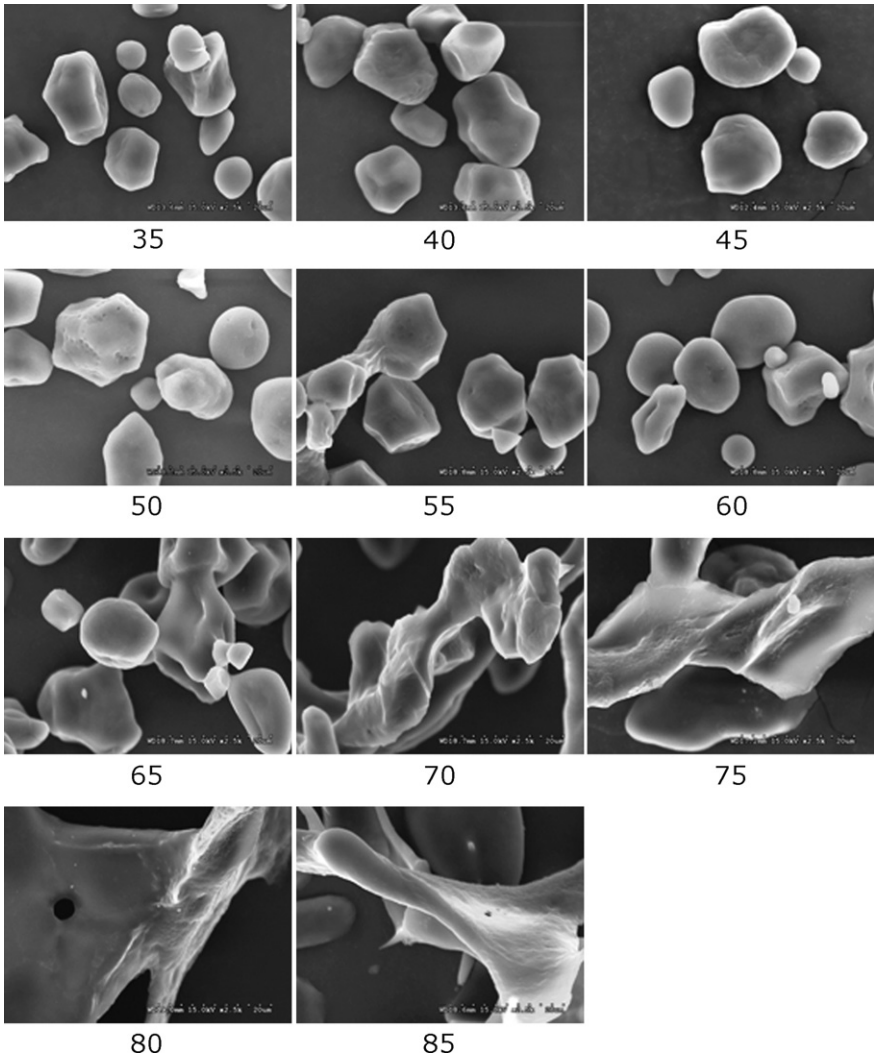

Fig. 3. SEM images of treated regular corn starch. The number below each figure represents the treatment temperature (°C). Magnification, 2500×.

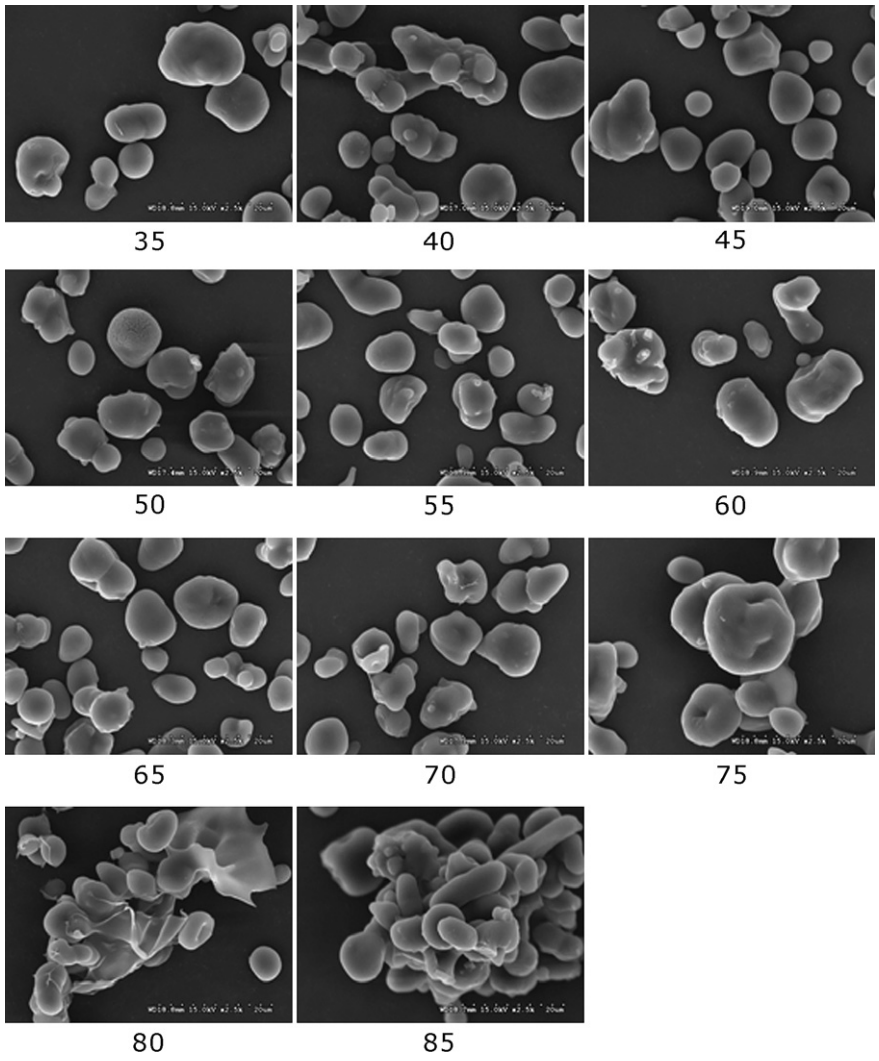

Fig. 4. SEM images of treated high-amylose corn starch. The number below each figure represents the treatment temperature (°C). Magnification, 2500×.

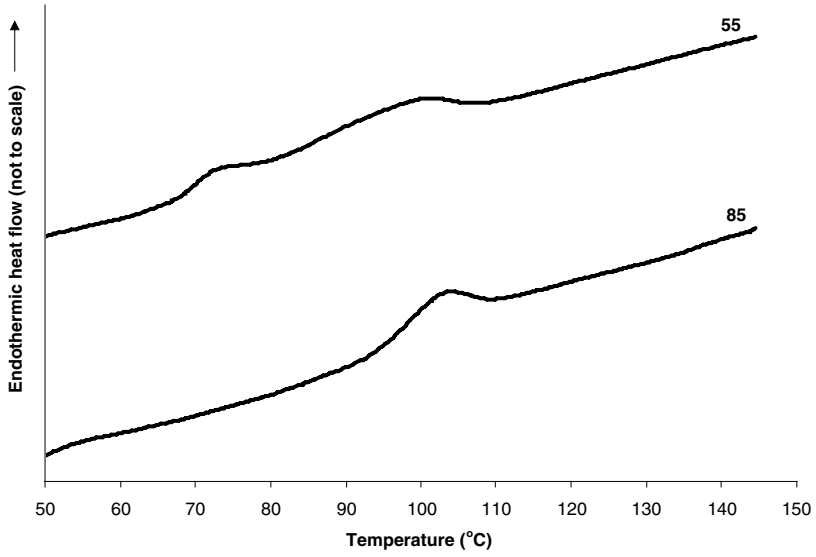

Fig. 5. Differences in DSC endotherms in high amylose corn starch samples treated at low (35–65 °C) and high (70–85 °C) temperatures. The numbers above each profile represent treatment temperatures.

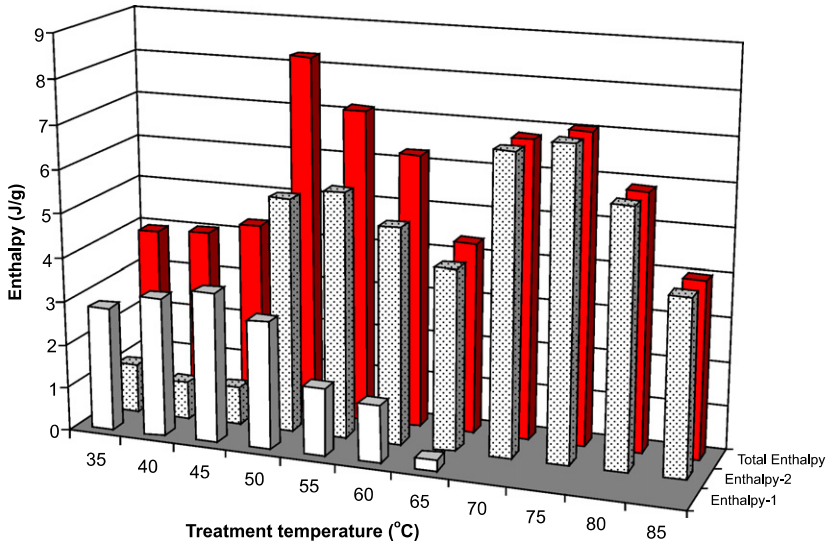

Fig. 6. Representative DSC enthalpies of heat treated high-amylose corn starch (the standard deviations for each series were in the ranges 0.03–0.40 for enthalpy-1, and 0.13–0.55 for enthalpy-2).

3.1. Regular corn starch

DSC enthalpies of treated regular corn starch samples increased from ~14 J/g at 35 °C to ~16.5 J/g at 50 °C in a linear fashion [$y = 0.156x + 8.65$ ($R^2 = 0.93$, $p = 0.03$), where x = treatment temperature (°C), and $y = \Delta$H (J/g)] (Fig. 1). The transition temperature range (T_c–T_o) decreased progressively over increasing treatment temperature. These DSC trends, taking place in regular corn starch just before granular disruption, are different from what is characterized as annealing. Annealing is a process by which a material is held at a temperature somewhat lower than its melting temperature, permitting modest molecular reorganization and a more organized structure of a lower free energy to form (Blanshard, 1987). Annealing is characterized by narrowed transition temperature ranges (T_c–T_o), increased gelatinization peak temperatures (T_p), and increased enthalpies (ΔH) of annealed starches compared to their native counterparts (Gomes, da Silva, Ricardo, Sasaki, & Germani, 2004; Lineback, 1986; Tester & Morrison, 1990). The DSC parameters observed in treated samples between 35–55 °C do not comply with the changes expected in annealing. The DSC parameters of untreated corn starch used in this study were: $T_o = 69.94$ °C, $T_p = 75.21$ °C, $T_c = 81.53$ °C, $(T_c - T_o) = 11.59$ °C, and ΔH = 15.34 J/g. It is likely that the energy provided before the initiation of granular disruption causes formation of new, but less stable, molecular interactions within granules which result in progressively lower DSC peak temperatures between 45 and 55 °C treatments (Appendix A1). In HPSEC profiles, the amounts of amylose dispersed decreased from the 35 °C to the 70 °C treatments. This may be attributed to the increased role of amylose in the proposed structural rearrangement occurring within the granules before their breakdown during the process. HPSEC results (Tables 2 and 3) also suggest that neither amylose nor amylopectin molecular structures are changed during treatment processes. The relative crystallinity of regular corn starch gradually decreased from 30% (at 35 °C) to ~3% (at 75 °C) and completely disappeared at 80 and 85 °C (Fig. 2). This suggests that the new molecular rearrangements that took place between 35 and 55 °C treat-

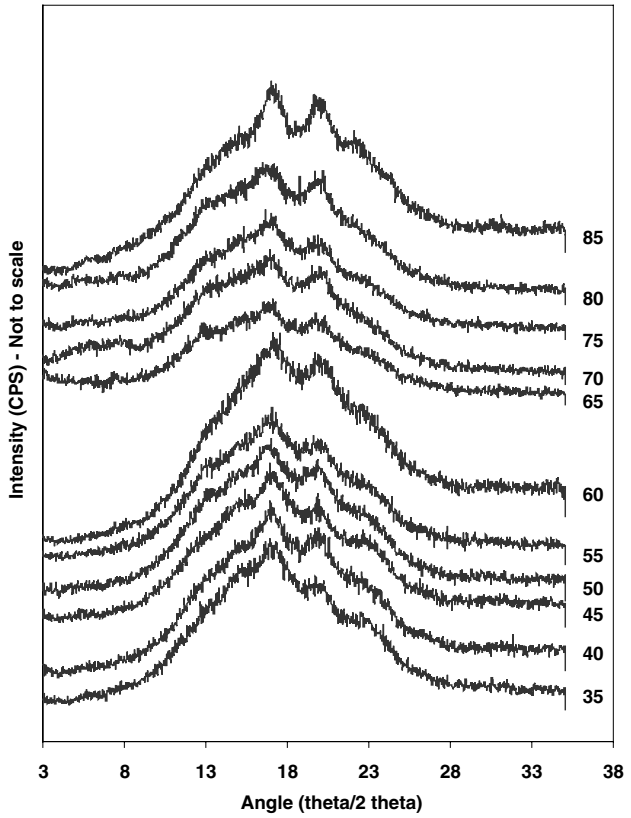

Fig. 7. Representative XRD patterns of high-amylose corn starch. Numbers to the right of each profile represent the corresponding treatment temperature (°C).

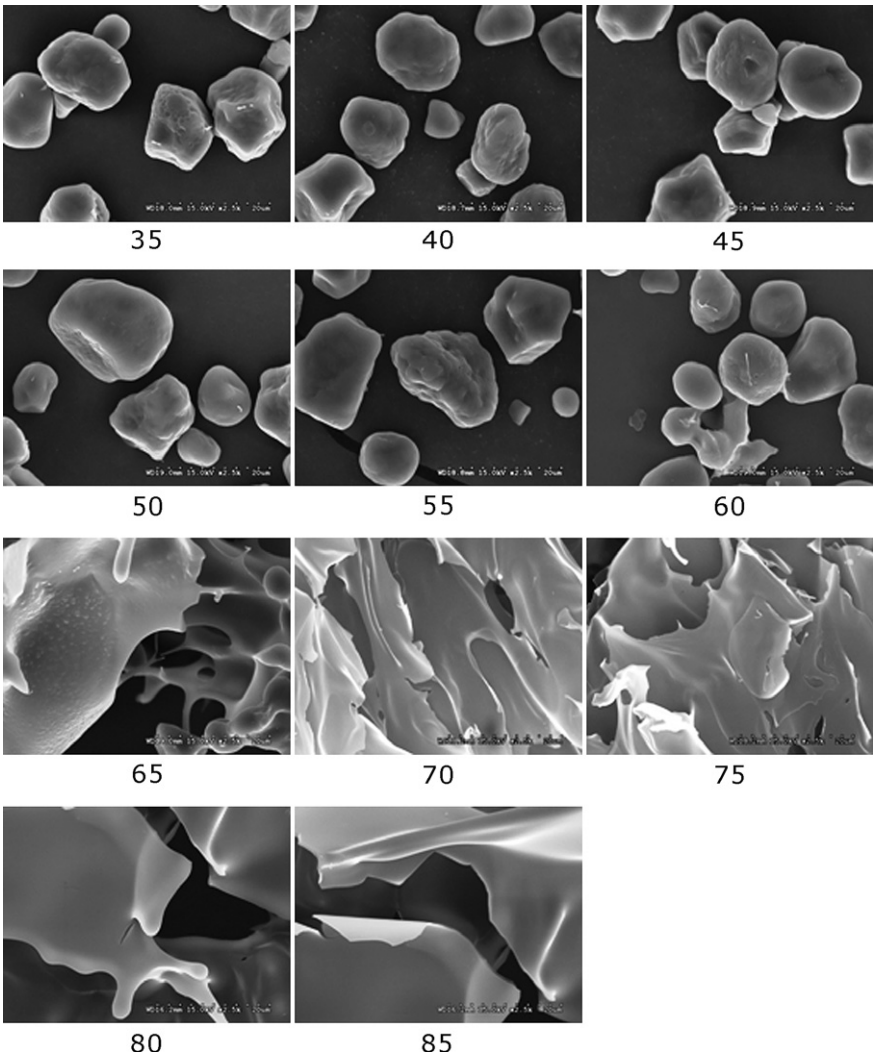

Fig. 8. SEM images of treated waxy corn starch. The number below each figure represents the treatment temperature (°C). Magnification, 2500×.

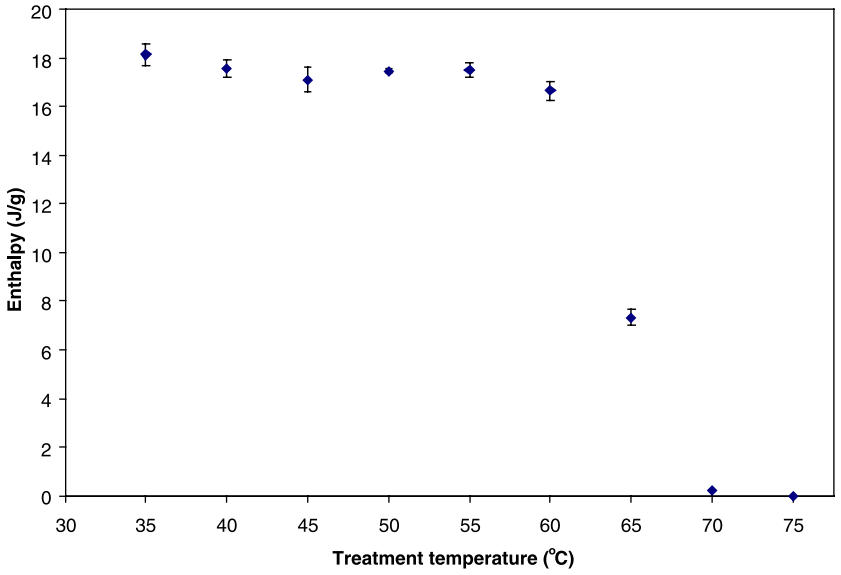

Fig. 9. Representative DSC enthalpies of waxy corn starch samples heated to specific temperatures (each data point represents the mean and standard deviation of three independent replicates). Temperatures above 70 °C did not yield enthalpies.

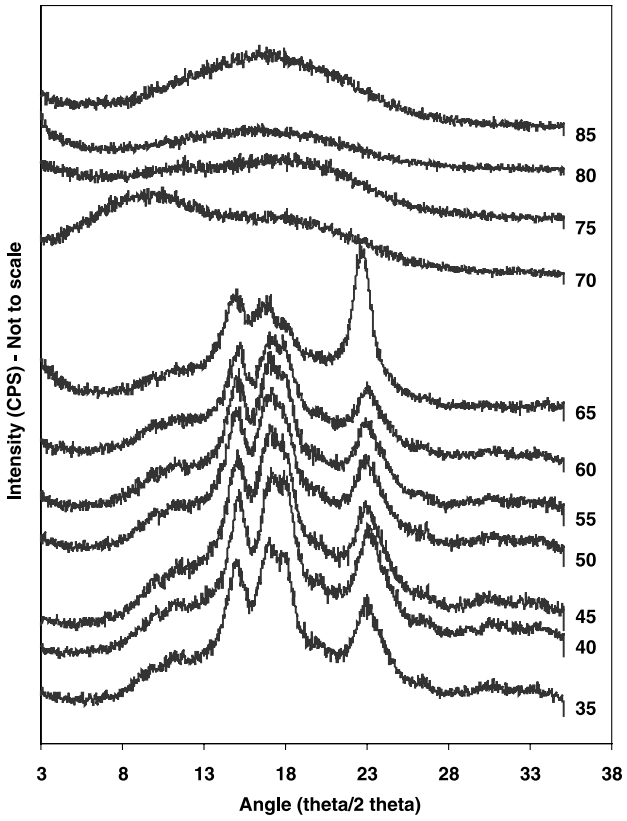

Fig. 10. Representative XRD patterns of waxy corn starch. Numbers to the right of each profile represent the corresponding treatment temperature (°C).

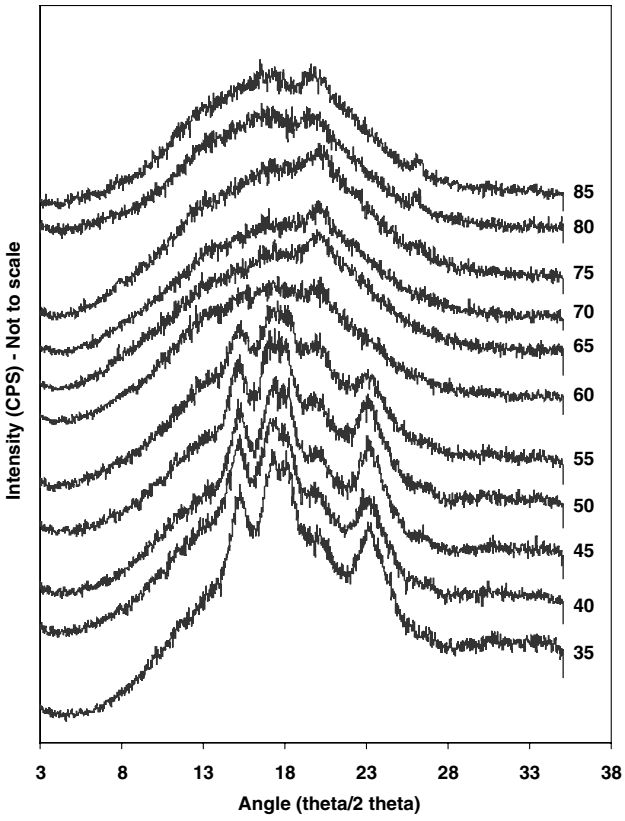

Fig. 12. Representative XRD patterns of wheat starch. Numbers to the right of each profile represent the corresponding treatment temperature (°C).

ments did not contribute to the overall crystallinity of the granule. Also, these structural changes do not significantly alter granular morphology as observed by SEM (Fig. 3) and real-time light microscopy (Table 1).

3.2. High amylose corn starch

High amylose corn starch did not show granular swelling, at the temperatures studied (Fig. 4, Table 1),

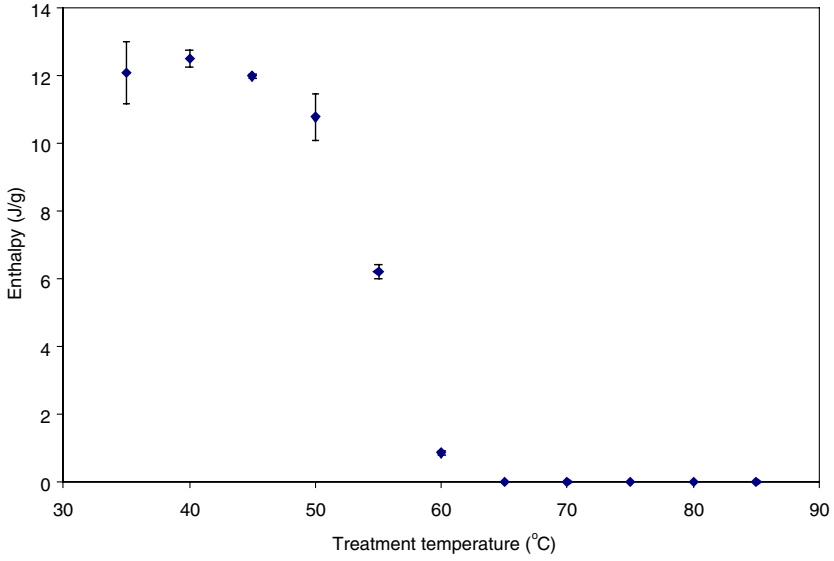

Fig. 11. Representative DSC enthalpies of wheat starch samples heated to specific temperatures (each data point represents the mean and standard deviation of three independent replicates).

indicating the necessity of higher amylopectin amounts for swelling process to occur. In the samples treated to specific temperatures, the DSC endotherms were bimodal in 35–65 °C treatments and only the second (high temperature, i.e., $T_p \sim 100$ °C) endotherm appeared in samples treated at 70–85 °C (Fig. 5 and Appendix A2). In the bimodal enthalpies, the peak temperatures (T_p) were ~74 °C in 35–60 °C treated samples and T_p was ~79 °C for the 65 °C treated sample. The high-temperature endotherms' T_p values were consistently at ~100 °C in all treatments. The variations in DSC enthalpies of high-amylose corn starch samples are illustrated in Fig. 6. The total enthalpy value increased gradually from 35 to 45 °C treatments, and then increased markedly at 50 °C (Fig. 6) while transition temperature range (T_c–T_o) and peak temperatures (T_p) remained essentially unchanged (data not shown). The results suggest that the structural changes took place during increasing heat treatments were different from annealing. It also is evident that there are two distinctly different groups of intermolecular bonds present in low temperature (35–65 °C) treated high-amylose corn starch samples, and just one such group is present in high temperature (65–85 °C) treated samples. It is possible that high temperature treatments destroyed less stable intermolecular bonds while not affecting the second – high stability – group of bonds. This phenomenon was not observed in the other starches examined in this study. The relative crystallinity gradually increased from ~19% at 35 °C to a highest value of 32% at 65 °C treatment and then decreased to ~23% at 85 °C (Fig. 7). Shamai, Shimoni, and Bianco-Peled (2004) reported, using small angle X-ray diffraction, that gelatinization disrupted the crystalline structure of high amylose corn starch. They studied enzyme treated high-amylose corn starch samples (resistant starch) treated at 121 °C for 120 min in an autoclave, but did not investigate the structural changes at low temperatures before gelatinization.

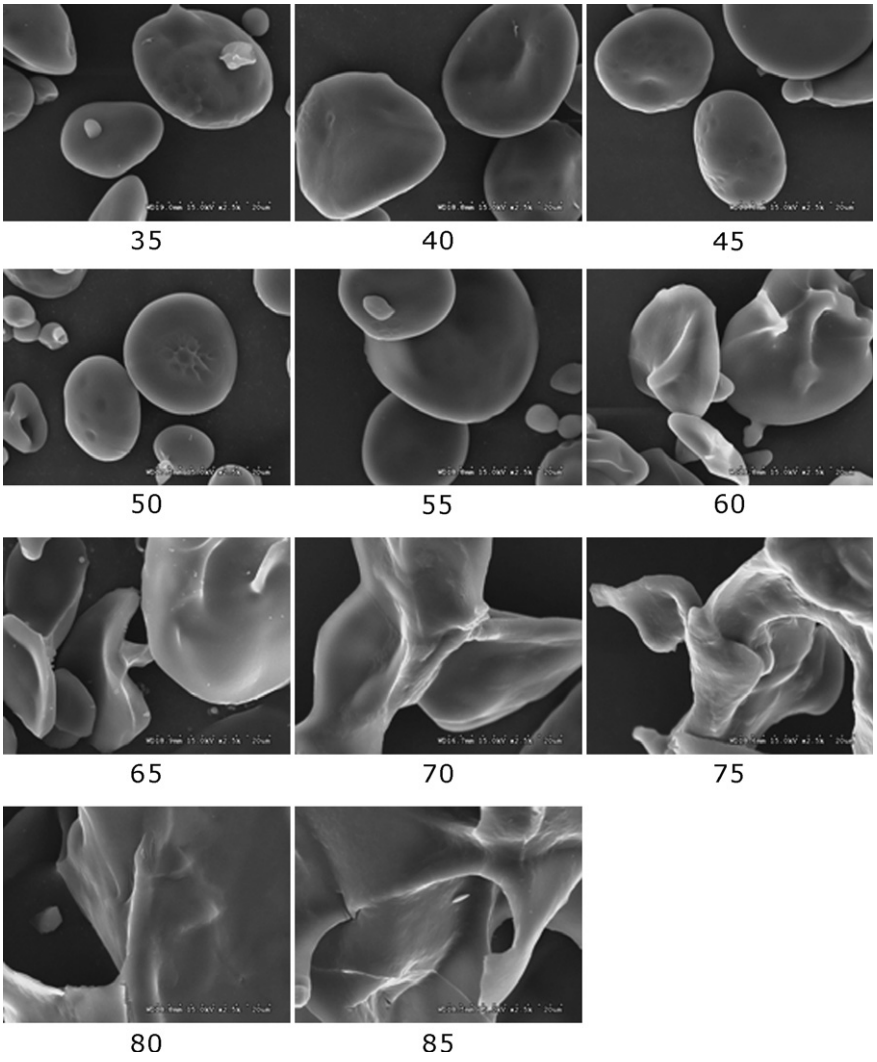

Fig. 13. SEM images of treated wheat starch. The number below each figure represents the treatment temperature (°C). Magnification: 2500×.

3.3. Waxy corn starch

Waxy corn starch granules stayed visibly intact until 55 °C and started to swell at 60 °C (Fig. 8 and Table 1). DSC enthalpy values quickly dropped to zero when treated above 60 °C and more or less unchanged below 60 °C treatments (Fig. 9 and Appendix A3). Shi and Seib, (1992) reported that annealing increased T_o and significantly decreased ΔH in DSC profiles. The enthalplic results observed here are not consistent with their observations and, therefore, it can be concluded that the effect of these particular low temperature treatments, up to 60 °C, on waxy corn starch granules is different from annealing. In contrast to regular corn starch, these results suggest that there were no considerable molecular rearrangements occurring within waxy corn starch granules before they were disrupted by increasing hydrothermal treatment (>65 °C). The relative crystallinity of waxy corn starch increased from 23% at 35 °C to 36% (significant at $p < 0.05$) at 45 °C and disappeared over increasing temperatures (>75 °C resulted in 0%) (Fig. 10). There were no significant ($p < 0.05$) differences (either in relative amounts of polymers dispersed or molecular weights) among HPSEC profiles of treated waxy corn starch samples. All profiles had one peak (Table 3) which estimated a molecular weight of 3.03×10^7. These results confirm the greater role of amylose in the structural changes that took place in regular corn starch. Furthermore, the structural changes that occur prior to and during gelatinization processes in waxy corn starch, before complete granule disruption, are vastly different from those of regular and high-amylose corn starches.

3.4. Wheat starch

Wheat starch showed gradual changes in granular morphology as heat treatment temperature increased. The results observed in wheat starch at 80–85 °C are in accordance with those of Conde-Petit, Nuessli, Handschin, and Escher (1998). DSC enthalpies rapidly disappeared

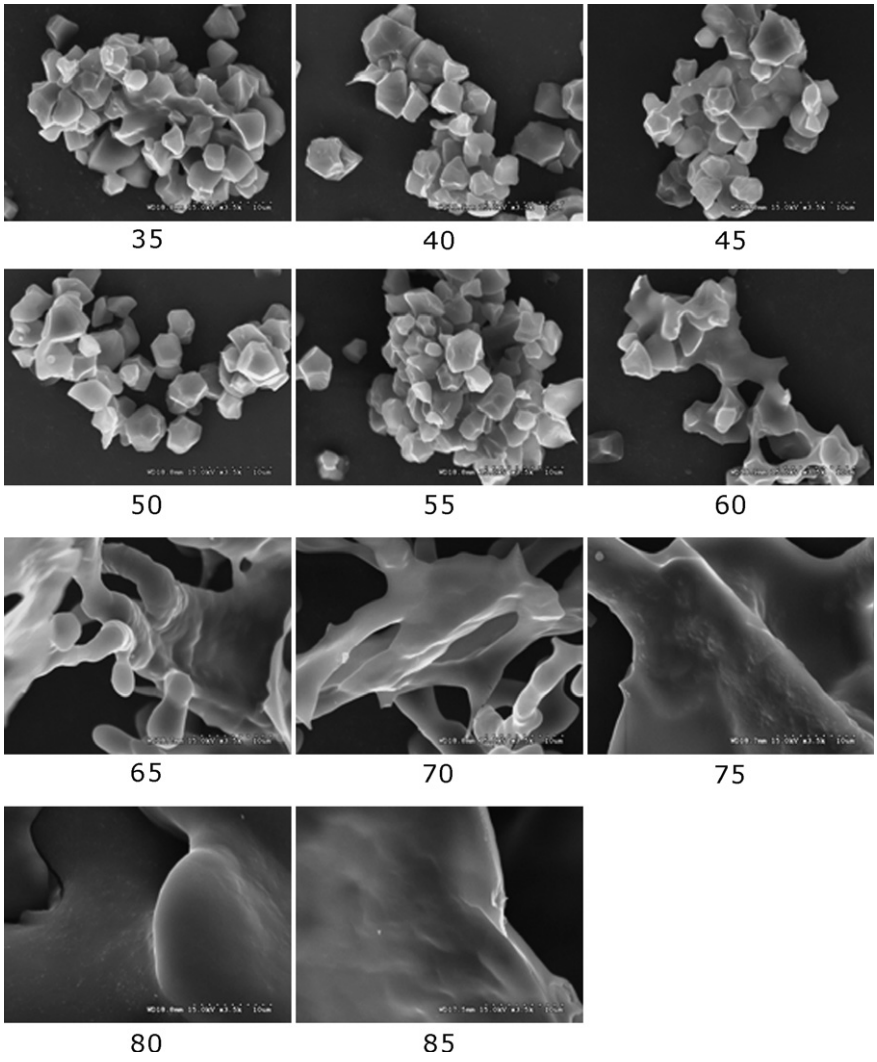

Fig. 14. SEM images of treated rice starch. The number below each figure represents the treatment temperature (°C). Magnification, 2500×.

between 50 and 60 °C treatments (Fig. 11 and Appendix A4). Gough and Pybus (1971) observed an increase in gelatinization enthalpy in annealed wheat starch at 50 °C for 72 h. They suspected a structural change of some sort is responsible for this observation, although it was not explained what exact structural changes took place in the annealed samples. Chiotelli and Le Meste (2002) reported comparable (8.1–14.3 J/g) ΔH values for native wheat starch. These authors also reported that large and small granules behaved differently during gelatinization, i.e., small granules gelatinize at high temperatures compared to large granules. Real-time light microscopic results (Table 1) are in agreement with their reports. The relative crystallinity gradually decreased from ~20% to 0% as samples were treated from 35 to 85 °C. Samples heated to above 60 °C were completely amorphous (Fig. 12). Tester and Morrison (1994) studied thermal behavior of hydrothermally treated wheat starch at 20, 40, 60, and 80 °C for 30 min in water. They reported that gelatinization and swelling were positively influenced by the treatment. Cooke and Gidley (1992) observed a complete loss of crystalline order in wheat starch (5% w/v in water) heated to 59 °C (time unspecified). From the microscopic data (Table 1 and Fig. 13) it can be concluded that irreversible swelling of granules (note: 60 °C treatment) during gelatinization process completely disrupted the crystalline order detected by wide-angle X-ray diffraction (Fig. 12).

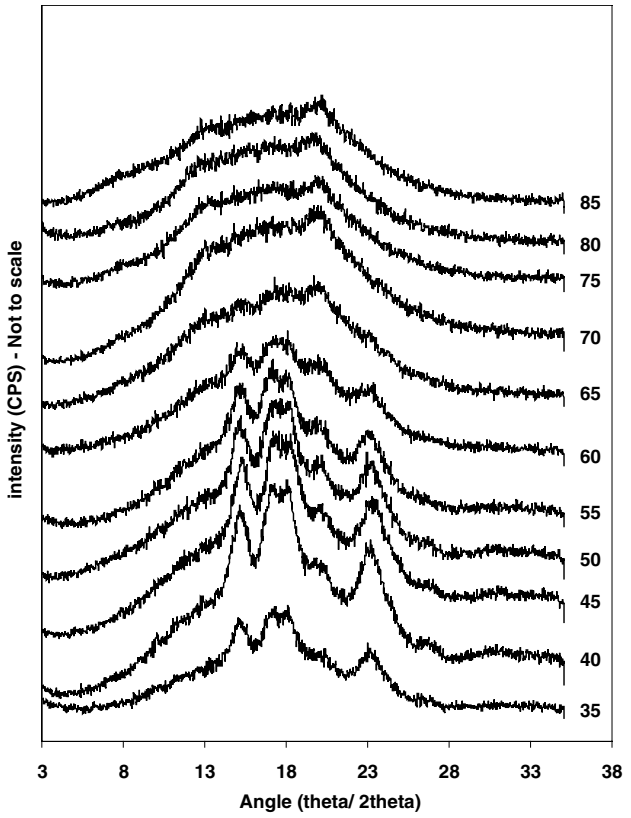

Fig. 15. Representative XRD patterns of rice starch. Numbers to the right of each profile represent the corresponding treatment temperature (°C).

3.5. Rice starch

Microscopic studies revealed that irreversible granular swelling occurs in rice starch around 60 °C (Fig. 14 and Table 1). Ramesh, Mitchell, Jumel, and Harding (2000), by HPSEC and gel-permeation chromatography studies, reported that rice starch contained far less amounts of amylose than previously reported in literature. Presence of less amylose may be another reason for the observed less swelling before granular disruption during heating. The crystallinity was completely lost at 70 °C (Fig. 15). The percent relative crystallinity gradually decreased from ~20%

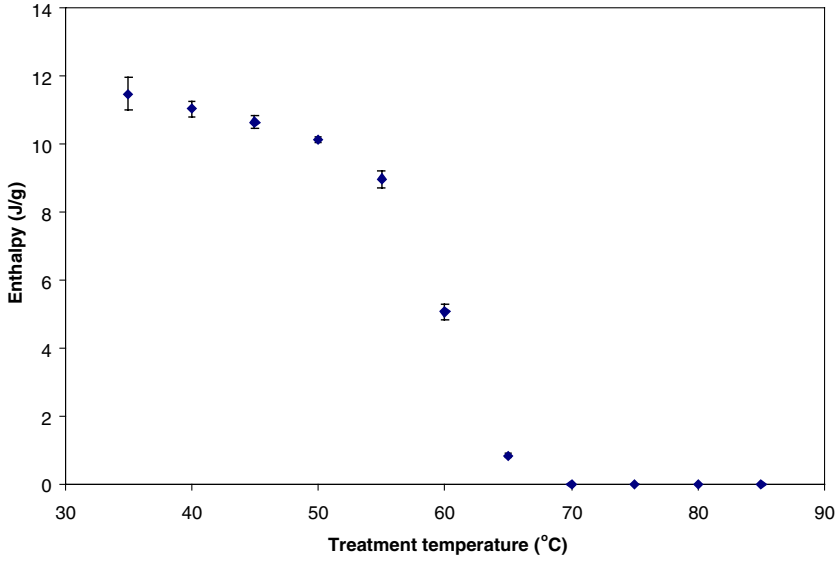

Fig. 16. Representative DSC enthalpies of rice starch samples heated to specific temperatures (each data point represents the mean and standard deviation of three independent replicates).

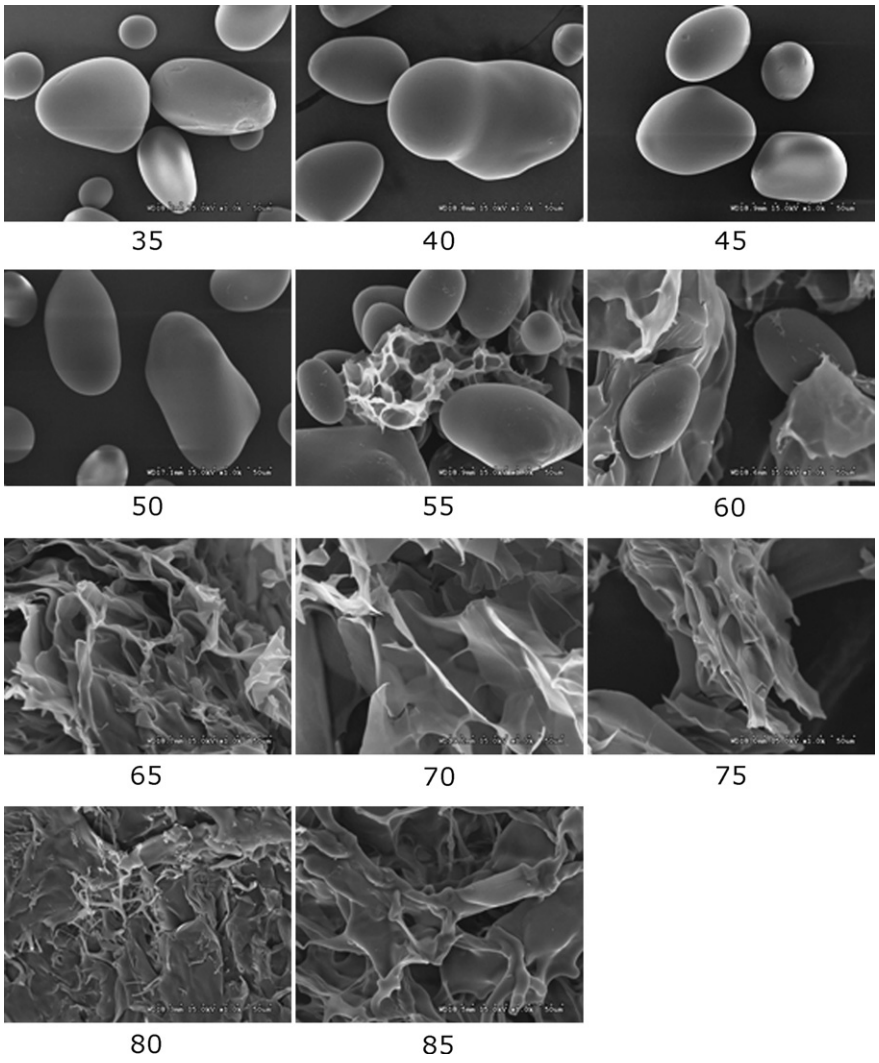

Fig. 17. SEM images of treated potato starch. The number below each figure represents the treatment temperature (°C). Magnification, 1000×.

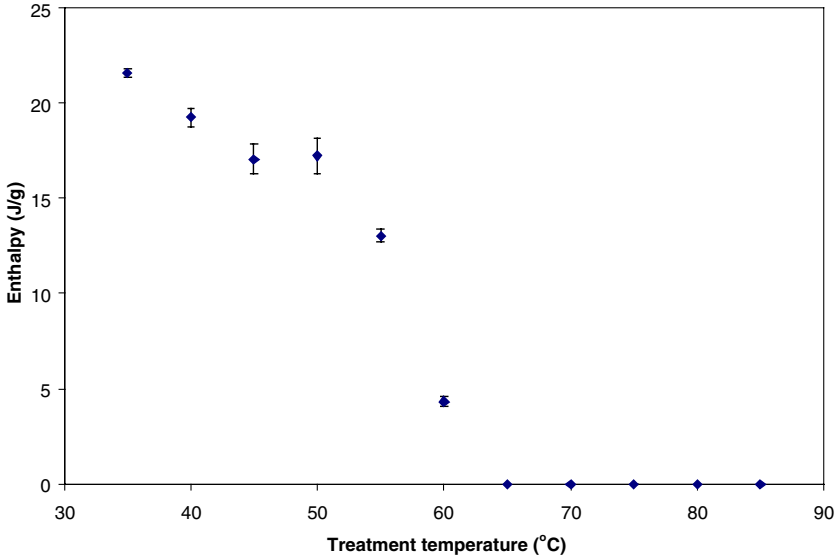

Fig. 18. Representative DSC enthalpies of potato starch samples heated to specific temperatures (each data point represents the mean and standard deviation of three independent replicates).

to ~10% from 35 to 65 °C. It has been reported that rice starch has lower crystallinity compared to other starches (Bao & Bergman, 2004). Starch became completely amorphous at treatments above 70 °C (Fig. 15). The loss of DSC enthalpy was gradual from 35 to 55 °C and then sudden between 60 and 70 °C (Fig. 16). The transition temperature range (T_c–T_o) decreased from ~16.70 °C at 35 °C to ~9.60 °C at 65 °C treatment while T_p increased from ~69.35 °C at 35 °C to ~77.70 °C at 65 °C (Appendix A5). Thirathumthavorn and Charoenrein (2005) observed a decreasing trend in DSC enthalpy in rice starch with increasing degree of acid hydrolysis (1 M hydrochloric acid at 35 °C, from 0 to 48 h) indicating the important role of amorphous regions of the granules in gelatinization. The results of this investigation suggest that the pre-gelatinization structural changes in rice starch granules were gradual and depended on the intensity of heating. It is important to note that rice starch granules are compound granules (Fig. 14) and they tend to gradually dissociate during heating. This dissociation of compound granules also may have contributed to some of the results observed here.

3.6. Potato starch

The microscopic results (Table 1 and Fig. 17) observed in potato starch at 80–85 °C were in accordance with those of Conde-Petit et al. (1998). Irreversible granular swelling occurred between 60 and 65 °C (Fig. 17) treatments. Permanent structural damage, observed as loss of crystallinity, also occurred within the same temperature range. Cooke and Gidley (1992) reported complete loss of crystallinity, molecular order, and DSC enthalpy in potato starch samples treated to 67 °C in excess water. The results in this study also are consistent with their observations. Although the loss of DSC enthalpy was gradual (Fig. 18 and Appendix A6), the loss of crystallinity was sudden between 55 and 60 °C (Fig. 19). The relative crystallinity was ~45% for all treatments from 35 to 55 °C and it suddenly dropped to ~10% at 60 °C and disappeared in >65 °C treatments (Fig. 19). HPSEC results did not demonstrate visible trends, i.e., varied widely, in the relative amounts of amylose and amylopectin dispersed among different treatments (data not shown). The profiles consistently yielded two identical peaks (Table 3). These results suggest that the pre-gelatinization structural changes in potato starch granules were either not as pronounced as in other starches or not clearly detectable by the techniques used in this study.

3.7. Tapioca starch

It has been reported that tapioca (cassava) starch crystallinity, molecular order, and DSC enthalpy were completely lost at ~69.5 °C upon heating in water (Cooke & Gidley, 1992). In this study, irreversible granular swelling occurred at 70 °C (Table 1 and Fig. 20). In treated samples, the relative crystallinity was 31% in the treatments between 35 and 60 °C. It dropped to ~10% at 65 °C and the samples

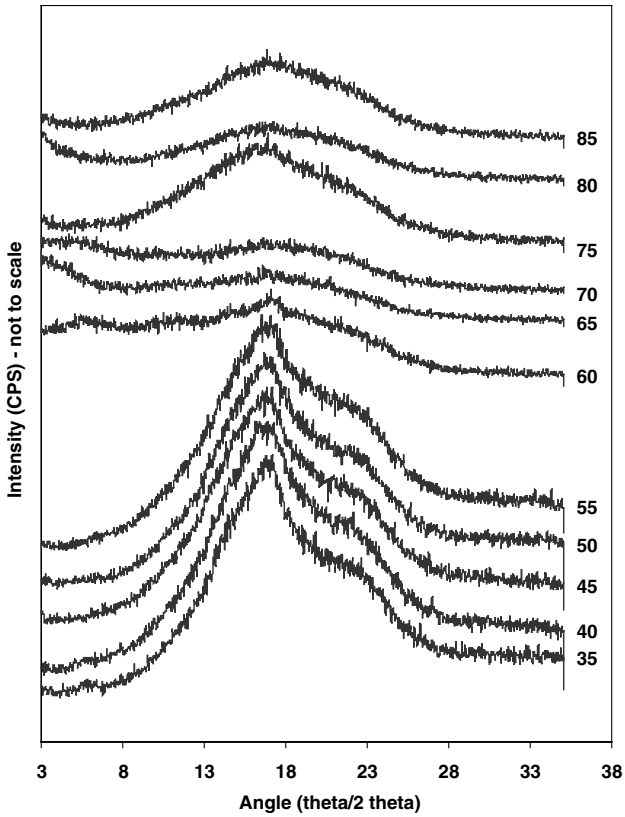

Fig. 19. Representative XRD patterns of potato starch. Numbers to the right of each profile represent the corresponding treatment temperature (°C).

treated between 70 and 85 °C were completely amorphous (Fig. 21). The DSC enthalpy slightly decreased from 35 to 60 °C and then rapidly dropped from 60 to 70 °C (Fig. 22). The transition temperature range (T_c–T_o) decreased from ~17.36 °C at 35 °C to ~11.72 °C at 60 °C while T_p remained essentially unchanged (Appendix A7). HPSEC results indicated the absence of molecular weight changes during the gelatinization process and there were no changes in the relative amounts of amylose and amylopectin dispersed at each treatment temperature (data not shown).

4. Conclusions

The granular structural changes that took place during the phase transition of the investigated starches reveals that starch gelatinization is a more complex process than the previously suggested order-to-disorder transition. The starch phase transition process is a series of events that occur progressively; it is definitely not a sudden or "quick" process that takes place within a narrow temperature range. Attempts to explain starch phase transitions just by examining only DSC or microscopic data might lead to an incomplete understanding of the phenomena. It is evident when gelatinization takes place using the conditions studied, that the gelatinization process initiates at low temperatures and continues until the granules are completely disrupted.

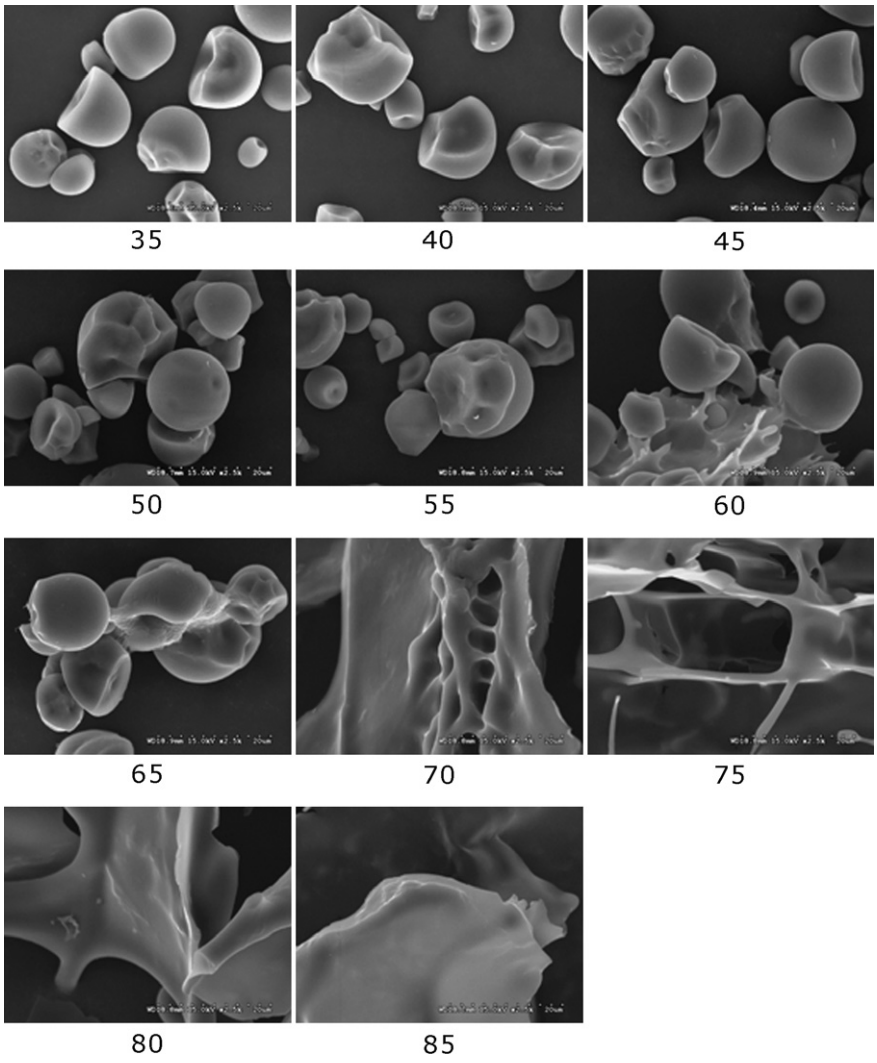

Fig. 20. SEM images of treated tapioca starch. The number below each figure represents the treatment temperature (°C). Magnification, 2500×.

A shortcoming of some previously published starch gelatinization models is that the observations used to construct various theories were mainly based on DSC results. DSC enthalpies represent all endothermic reactions that take place within the given transition temperature range. Therefore, subjecting native starch granules to DSC experiments reveals limited information about changes in polymer structures that occur at specific temperatures. Changes in starch structure that occur at low temperatures are rarely or difficult to observe using DSC, but are clearly observed using other techniques such as HPSEC and XRD. In our opinion, DSC should be used along with other techniques to identify all the aspects of gelatinization and phase transition associated structural changes in starch granules. By emphasizing mostly DSC data to explain gelatinization phenomena, researchers may underestimate the importance of amylose in phase transition associated structural changes in starch granule's amorphous regions. Our results suggest that the amorphous regions and amylose molecules located in those regions play a significant role in low temperature structural changes during phase transition.

During the first portion of the phase transition, water absorbed by starch granules increases the mobility of starch polymers, especially amylose in amorphous domains. The results suggest that the increased polymer mobility facilitates rearrangement of these polymers. This polymer rearrangement includes polymer realignment and formation of new intermolecular bonds. An increase in DSC enthalpy values with increasing lower-temperature thermal pre-treatments confirms this phenomenon. Changes in relative crystallinities, at low temperatures, suggest that the structural changes also include alterations in the crystalline domains of granules. These changes in crystalline order, measured by XRD, depend on starch type and they do not necessarily follow the same pattern of change observed in DSC enthalpies. Changes in amorphous and crystalline domains occur simultaneously during any initial low temperature heat treatments. We do not, however, have conclusive evidence from this study indicating if the changes in the two domains are dependent or independent of each other.

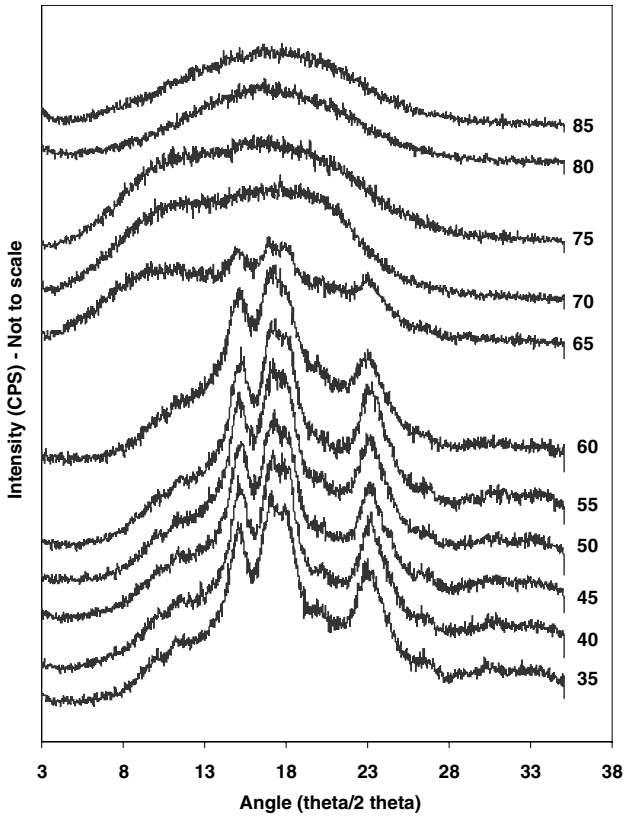

Fig. 21. Representative XRD patterns of tapioca starch. Numbers to the right of each profile represent the corresponding treatment temperature (°C).

Upon further heating, at increased temperatures, starch polymers become more mobile, reduce or lose their interpolymer interactions, and starch granules break apart (except in high amylose starch heated to <85 °C). The initiation and progression of this portion of the phase transition process is detectable by microscopy and DSC. Microscopy and XRD results suggest that the sources of DSC endotherms' specific patterns result from differences in intermolecular interactions as well as overall granular stabilities, i.e., some granules of regular corn, wheat, rice, potato, and tapioca starches seem to be somewhat more stable at increasing hydrothermal treatments.

In summary, it can be concluded that starch phase transitions are three stage processes during which the following structural events take place: (1) water absorption by starch granules facilitates increased starch polymer mobility in the amorphous regions, (2) starch polymers in the amorphous regions rearrange often forming new intermolecular interactions, and (3) with increasing hydrothermal effects, the polymers become more mobile and lose their intermolecular interactions and overall granular structure. The energy absorbed by granules not only melts crystallite structures during gelatinization, but also facilitates "rearrangement" or formation of new bonds among molecules at lower temperatures before gelatinization. An array of new molecular rearrangements and bonds having different stabilities is formed during this structural re-ordering process. This rearrangement process is different from annealing and the nature of this restructuring process, before granule breakdown, depends on the starch type.

Acknowledgments

The authors thank Dr. Kit Lee, Dr. You Zhou, Terri Fangman (Microscopy Core Facility, Beadle Center, University of Nebraska-Lincoln), and Brian Jones (Center for Materials Research and Analysis, Behlen Laboratory, University of Nebraska-Lincoln) for technical assistance in microscopy and XRD analyses.

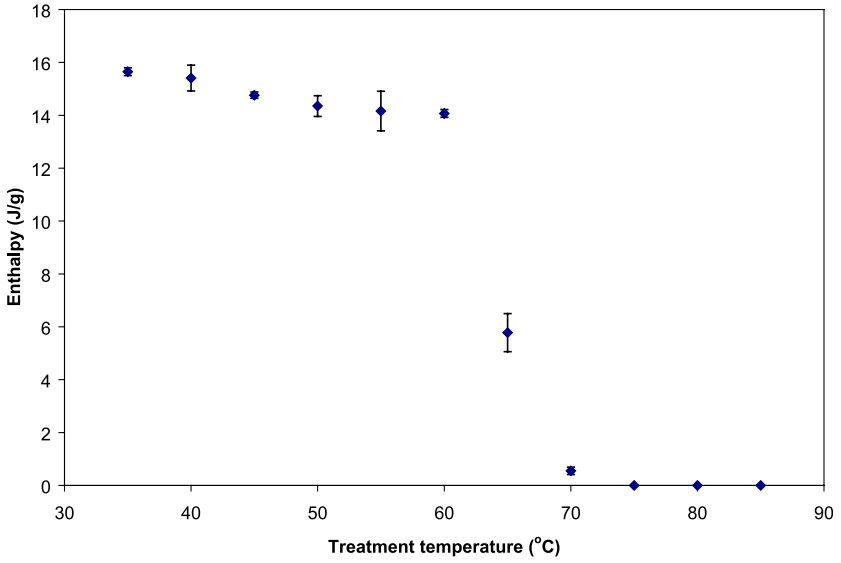

Fig. 22. Representative DSC enthalpies of tapioca starch samples heated to specific temperatures (each data point represents the mean and standard deviation of three independent replicates).

Appendix A

Figs. A1–A7.

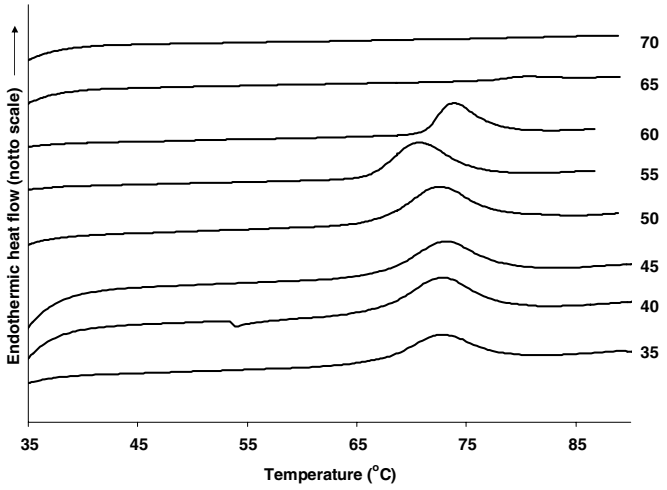

Fig. A1. Representative DSC profiles of regular corn starch heated to specific temperatures. The numbers next to profiles on the right represent treatment temperature (°C). Temperatures above 65 °C did not display endotherms.

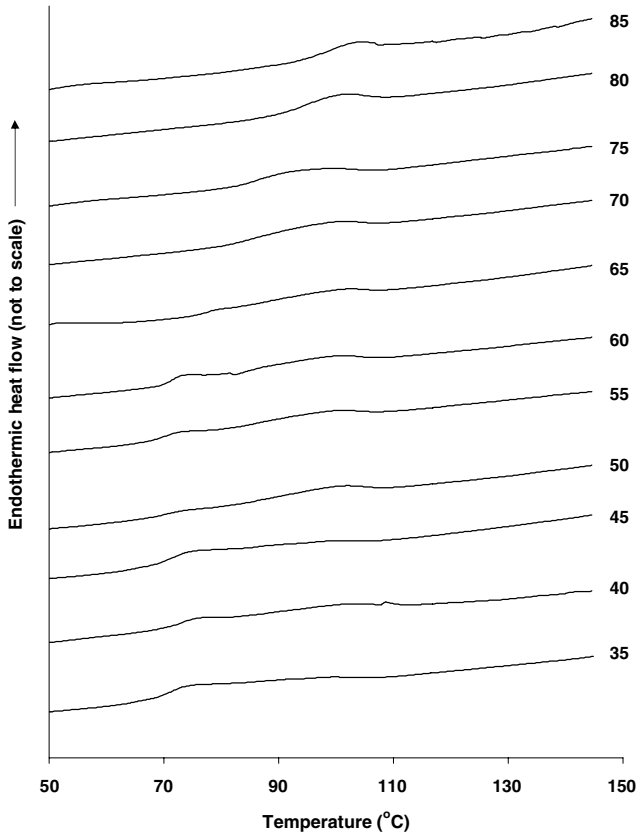

Fig. A2. Representative DSC profiles of high-amylose corn starch heated to specific temperatures. The numbers next to profiles on the right represent treatment temperature (°C).

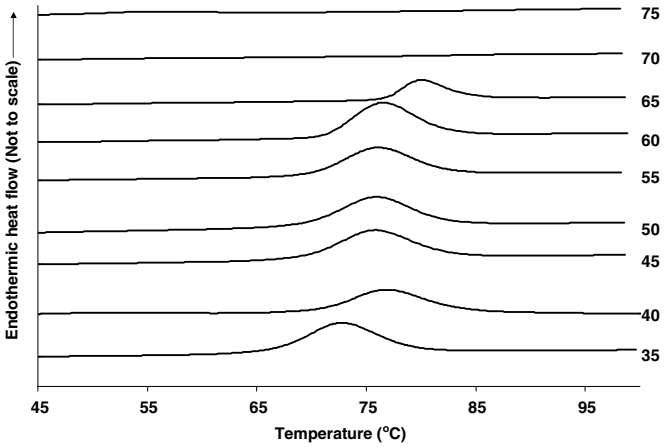

Fig. A3. Representative DSC profiles of waxy corn starch heated to specific temperatures. The numbers next to profiles on the right represent treatment temperature (°C). Temperatures above 75 °C did not display endotherms.

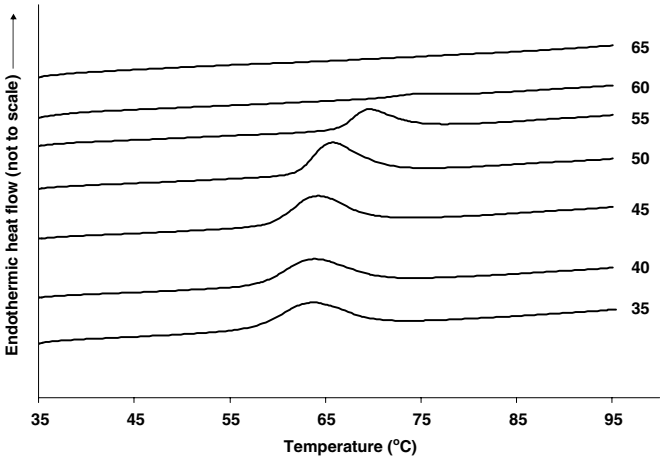

Fig. A4. Representative DSC profiles of wheat starch heated to specific temperatures. The numbers next to profiles on the right represent treatment temperature (°C). Temperatures above 65 °C did not display endotherms.

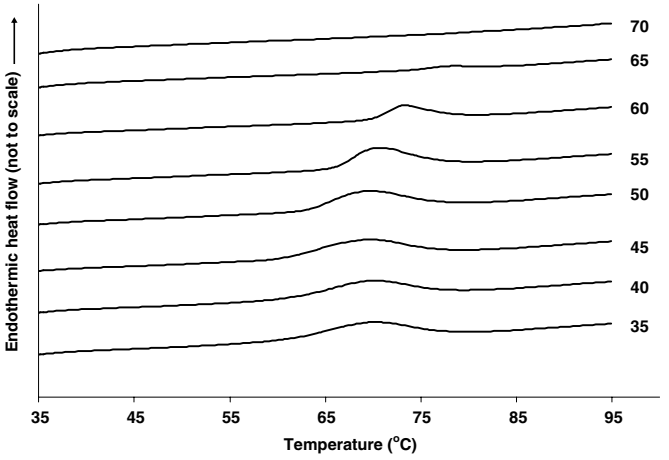

Fig. A5. Representative DSC profiles of rice starch heated to specific temperatures. The numbers next to profiles on the right represent treatment temperature (°C). Temperatures above 65 °C did not display endotherms.

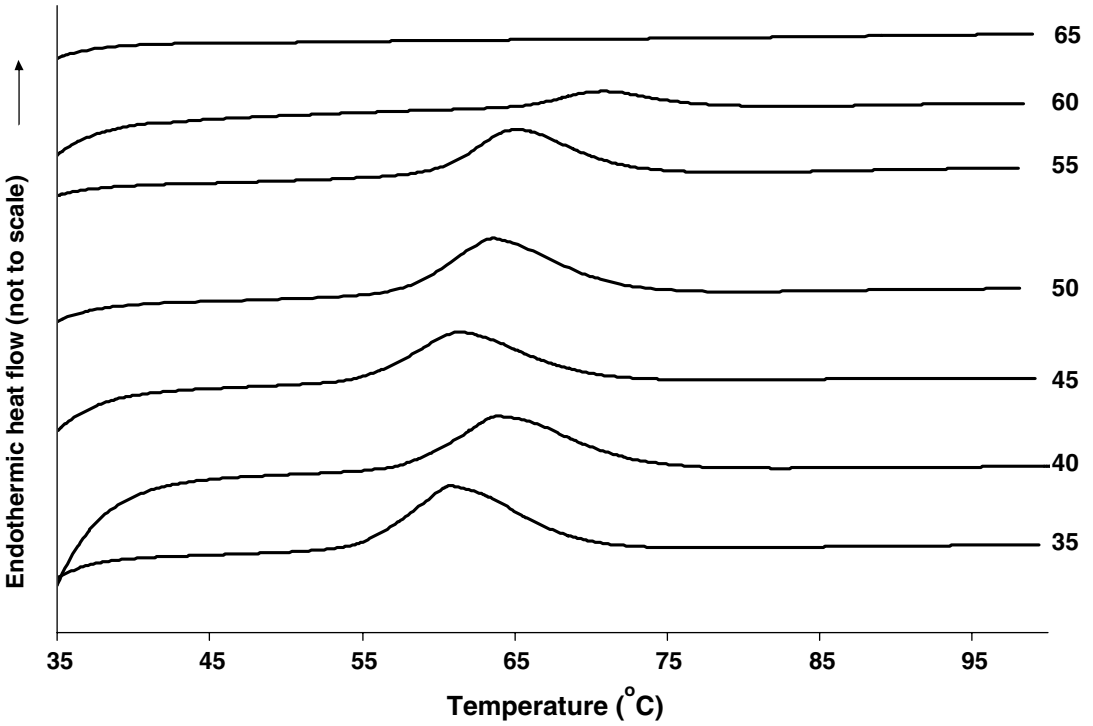

Fig. A6. Representative DSC profiles of potato starch heated to specific temperatures. The numbers next to profiles on the right represent treatment temperature (°C). Treatments above 65 °C did not yield endotherms.

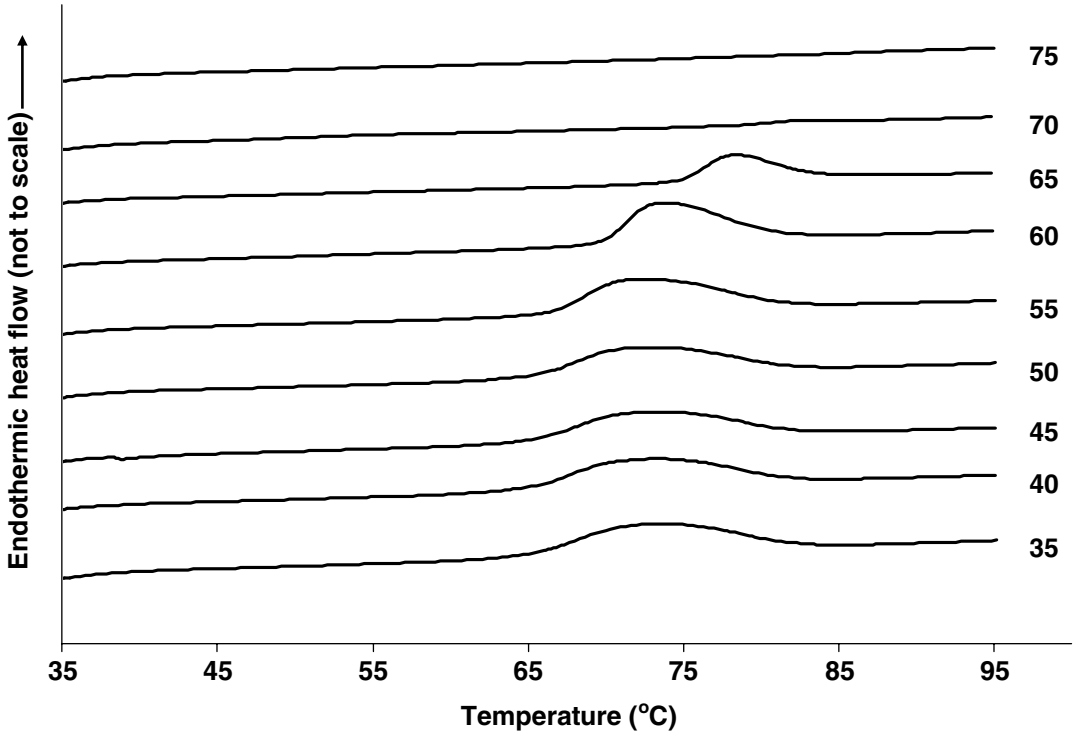

Fig. A7. Representative DSC profiles of tapioca starch heated to specific temperatures. The numbers next to profiles on the right represent treatment temperature (°C). Temperatures above 70 °C did not display endotherms.

Appendix B

Fig. B1.

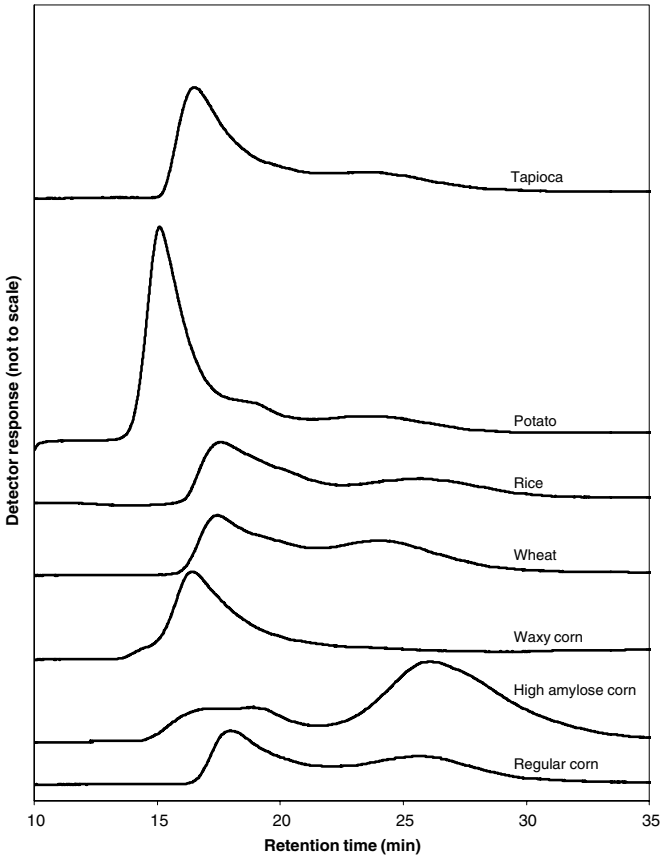

Fig. B1. Representative HPSEC profiles of treated (55 °C) starch samples. The first peak represents amylopectin and the second peak represents amylose in each profile.

References

Bao, J., & Bergman, C. J. (2004). The functionality of rice starch. In A.-C. Eliasson (Ed.), *Starch in food – structure function and applications* (p. 258). Cambridge: Woodhead Publishing Limited.

Biliaderis, C. G., Page, C. M., Maurice, T. J., & Juliano, B. O. (1986). Thermal characterization of rice starches: a polymeric approach to phase transition of granular starch. *Journal of Agricultural and Food Chemistry, 34*, 6–14.

Blanshard, J. M. V. (1987). Starch granule structure and function: a physicochemical approach. In T. Galliard (Ed.), *Starch: Properties and potential* (pp. 16). Chichester: John Wiley and Sons.

Chiotelli, E., & Le Meste, M. (2002). Effect of small and large wheat starch granules on thermomechanical behavior of starch. *Cereal Chemistry, 79*, 286–293.

Conde-Petit, B., Nuessli, J., Handschin, S., & Escher, F. (1998). Comparative characterisation of aqueous starch dispersions by light microscopy, rheometry and iodine binding behavior. *Starch/Stärke, 50*, 184–192.

Cooke, D., & Gidley, M. J. (1992). Loss of crystalline and molecular order during starch gelatinization: origin of the enthalpic transition. *Carbohydrate Research, 227*, 103–112.

Donovan, J. W. (1979). Phase transitions of the starch–water system. *Biopolymers, 18*, 263–275.

Eliasson, A. C., Larsson, K., Andersson, S., Hyde, S. T., Nesper, R., & von Schnering, H. G. (1987). On the structure of native starch – An analogue to quartz structure. *Starch/Stärke, 39*, 147–152.

Evans, I. D., & Haisman, D. R. (1982). The effect of solutes on the gelatinization temperature range of potato starch. *Starch/Stärke, 34*, 224–231.

Fukuoka, M., Ohta, K., & Watanabe, H. (2002). Determination of the terminal extent of starch gelatinization in a limited water system by DSC. *Journal of Food Engineering, 53*, 39–42.

Gomes, A. M. M., da Silva, C. E. M., Ricardo, N. M. P. S., Sasaki, J. M., & Germani, R. (2004). Impact of annealing on the physicochemical properties of unfermented cassava starch (“Polvilho doce”). *Starch/Stärke, 56*, 419–423.

Gough, B. M., & Pybus, J. N. (1971). Effect on the gelatinization temperature of wheat starch granules of prolonged treatment with water at 50 °C. *Die Stärke, 23*, 210–212.

Jenkins, P. J., & Donald, A. M. (1998). Gelatinization of starch: a combined SAXS/WAXS/DSC and SANS study. *Carbohydrate Research, 308*, 133–147.

Lineback, D. R. (1986). Current concepts of starch structure and its impact on properties. *Journal of the Japanese Society of Starch Science, 33*, 80–88.

Liu, Q., Charlet, G., Yelle, S., & Arul, J. (2002). Phase transition in potato starch–water system I. Starch gelatinization at high moisture level. *Food Research International, 35*, 397–407.

Marchant, J. L., & Blanshard, J. M. V. (1978). Studies of the dynamics of the gelatinization of starch granules employing a small angle light scattering system. *Starch/Stärke, 30*, 257–264.

Nakazawa, F., Noguchi, S., & Takahashi, J. (1984). Thermal equilibrium state of starch–water mixture studied by differential scanning calorimetry. *Agricultural and Biological Chemistry, 48*, 2647–2653.

Nara, S., Mori, A., & Komiya, T. (1978). Study on relative crystallinity of moist potato starch. *Starch/Stärke, 30*, 111–114.

Ozcan, S., & Jackson, D. S. (2002). The impact of thermal events on amylose-fatty acid complexes. *Starch/Stärke, 54*, 593–602.

Qi, X., Tester, R. F., Snape, C. E., & Ansell, R. (2005). The effect of annealing on structure and gelatinization of maize starches with amylose dosage series. *Progress in Food Biopolymer Research, 1*, 1–27.

Ramesh, M., Mitchell, J. R., Jumel, K., & Harding, S. E. (2000). What is the true amylose content of rice starch?. In P. A. Williams & G. O. Phillips (Eds.) *Gums and stabilisers for the food industry 10* (pp. 76–98). Cambridge: Royal Society of Chemistry.

Roos, Y. H. (1995). Food components and polymers. In S. L. Taylor (Ed.), *Phase transitions in foods* (pp. 109). San Diego CA: Academic Press.

Sahai, D., & Jackson, D. S. (1999). Enthalpic transition in native starch granules. *Cereal Chemistry, 76*, 444–448.

Sene, M., Thevenot, C., & Prioul, J. L. (1997). Simultaneous spectrophotometric determination of amylose and amylopectin in starch from maize kernel by multi-wavelength analysis. *Journal of Cereal Science, 26*, 211–221.

Shamai, K., Shimoni, E., & Bianco-Peled, H. (2004). Small angle X-ray scattering of resistant starch type-III. *Biomacromolecules, 5*, 219–223.

Shi, Y.-C., & Seib, P. A. (1992). The structure of four waxy starches related to gelatinization and retrogradation. *Carbohydrate Research, 227*, 131–145.

Tester, R. F., & Morrison, W. R. (1990). Swelling and gelatinization of cereal starches. I. Effects of amylopectin, amylose, and lipids. *Cereal Chemistry, 67*, 551–557.

Tester, R. F., & Morrison, W. R. (1994). Properties of damaged starch granules. V. Composition and swelling of fractions of wheat starch in water at various temperatures. *Journal of Cereal Science, 20*, 175–181.

Thirathumthavorn, D., & Charoenrein, S. (2005). Thermal and pasting properties of acid treated rice starches. *Starch/Stärke, 57*, 217–222.